

^{109}Ag and ^{29}Si NMR Investigations of Scalar Couplings and Relaxation on Cyclo-tetrakis[tri-*tert*-butoxysilanethiolatosilver(I)], $[(t\text{-C}_4\text{H}_9\text{O})_3\text{SiSAg}]_4$

A. Schwenk

Physikalisches Institut der Universität Tübingen, Germany

U. Piantini

Organisch-Chemisches Institut der Universität Zürich, Switzerland

W. Wojnowski

Department of Chemistry, Technical University of Gdańsk, Poland

Z. Naturforsch. **46a**, 939–946 (1991); received September 7, 1991

From the ^{29}Si NMR spectrum of $[(t\text{-BuO})_3\text{SiSAg}]_4$ with a partly resolved fine structure recorded at 9.4 T, the coupling constants $|J(^{29}\text{Si}, ^{109}\text{Ag})| = (4.49 \pm 0.04) \text{ Hz}$ and $|J(^{29}\text{Si}, ^{107}\text{Ag})| = (3.90 \pm 0.03) \text{ Hz}$ were derived. The ^{109}Ag spectra at 9.4 T and at 2.1 T are single lines without fine structure shifted to higher frequency by $\delta = (725.8 \pm 1.5) \text{ ppm}$ relative to the resonance of the Ag^+ ion in aqueous solution at infinite dilution. No hint of any $\{\text{Ag}, \text{Ag}\}$ -coupling can be derived from these spectra and from a comparison of the FID- and steady-state-signal intensities, i.e. $|J(\text{Ag}, \text{Ag})| < 1 \text{ Hz}$. This result is in contrast to the assumption of an $\text{Ag}-\text{Ag}$ bond to explain the spatial shift of the Ag atoms towards the centre of the alternating Ag_4S_4 -eight-membered central ring of the molecule. For the first time silver relaxation was investigated in a molecule. $T_1(^{109}\text{Ag})$ was determined at 9.4 T and at 2.1 T and at different temperatures to separate the contributions of different mechanisms: chemical shift anisotropy is the dominating one. $T_1 = 20.2 \text{ s}$ at 2.1 T and at 301 K in this molecule is shorter by nearly two orders of magnitude than T_1 of the Ag^+ ion in aqueous solution.

1. Introduction

The structure of the cyclo-tetrakis[tri-*tert*-butoxysilanethiolatosilver(I)] molecule was elucidated by X-ray diffraction, by mass-spectroscopy, and by ^{29}Si NMR [1]. The central $\text{Si}_4\text{S}_4\text{Ag}_4$ part of this $[(t\text{-C}_4\text{H}_9\text{O})_3\text{SiSAg}]_4$ molecule is pointed out in Fig. 1 in two different views; the *t*-BuO groups bonded to silicon are omitted for clarity, as the nuclei contained in these ligands do not play a role in the present ^{109}Ag NMR investigations. This is also why the abbreviation $[\text{SiSAg}]_4$ will be used in the following for the molecule under investigation.

In Fig. 1b, the view perpendicular to the central ring of the $[\text{SiSAg}]_4$ molecule, it is pointed out that this alternating S_4Ag_4 -eight-membered ring is not a square with sulphur atoms at the corners and silver atoms in the middle of the sides. Rather the silver atoms are shifted spatially towards the centre of this

ring. The angle $\text{S}-\text{Ag}-\text{S}$ with the angular point at the Ag atom is 172.3° (mean value). A similar structure was reported recently of the isomorphous copper compound, the tetrameric copper tri-*tert*-butoxysilanethiolate, $[(t\text{-C}_4\text{H}_9\text{O})_3\text{SiSCu}]_4$ [2]. The $\text{S}-\text{Cu}-\text{S}$ bond angle is here 172.8° .

One possible explanation of this spatial shift of the metal atoms towards the centre of the ring could be a silver-silver or a copper-copper bond between vicinal or between opposite metal atoms. Such binding interaction between Ag atoms was assumed by Jansen [3] in Ag(I) oxides with a high ratio of cations to oxygen to explain unusual structural features. Some physical and chemical properties of these compounds were cited to support this assumption of $\text{Ag}-\text{Ag}$ bonds. There is, however, up until now no striking proof for such binding $\text{Ag}-\text{Ag}$ interactions. ^{109}Ag NMR provides a decisive test for such $\text{Ag}-\text{Ag}$ bonds in $[\text{SiSAg}]_4$, namely the investigation of homonuclear and heteronuclear $\{^{109}\text{Ag}, ^{109}\text{Ag}\}$ and $\{^{109}\text{Ag}, ^{107}\text{Ag}\}$ scalar couplings, as both silver nuclei ^{107}Ag and ^{109}Ag have the spin $I = 1/2$ and therefore very narrow NMR

Reprint requests to Prof. A. Schwenk, Physikalisches Institut der Universität Tübingen, Morgenstelle 14, W-7400 Tübingen, Germany.

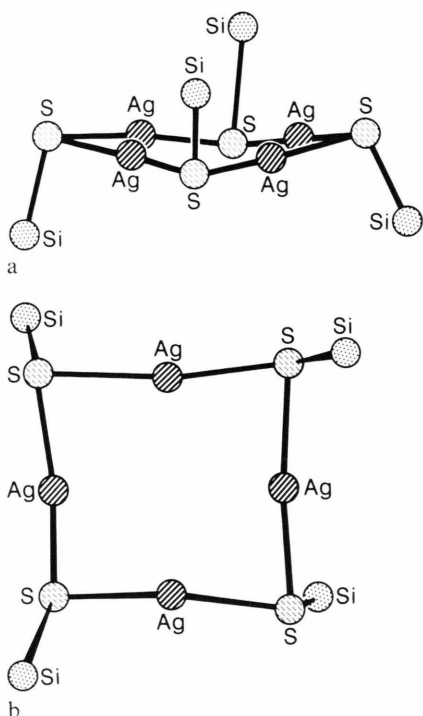


Fig. 1. The $\text{Si}_4\text{S}_4\text{Ag}_4$ core of the cyclo-tetrakis[tri-*tert*-butoxysilanethiolatosilver(I)] molecule (the 12 *t*-BuO ligands bonded to silicon are omitted). a) View nearly parallel to the central plane defined by the four silver atoms. The 4 sulphur atoms are alternatingly slightly below and above this plane. b) View perpendicular to the central Ag_4 plane. The eight-membered Ag_4S_4 ring is not a square, rather the four Ag atoms are shifted towards the centre of the ring. (Angle $\text{S}-\text{Ag}-\text{S} = 172.3^\circ$).

lines due to the missing quadrupole interaction. Similar investigations of couplings on the isomorphous copper compound $[\text{SiSCu}]_4$ will fail because of the wide copper lines due to the quadrupole interaction of both copper nuclei ^{63}Cu and ^{65}Cu with spin $I = 3/2$. Silver-silver coupling constants $^1J(^{109}\text{Ag}, ^{109}\text{Ag})$, $^1J(^{109}\text{Ag}, ^{107}\text{Ag})$, and $^1J(^{107}\text{Ag}, ^{107}\text{Ag})$ were determined with the aid of INEPT-techniques by Brown et al. [4] in the range of 40 Hz. Homonuclear and heteronuclear $\{\text{Ag}, \text{Ag}\}$ couplings weaker even more than one order of magnitude could be detected easily in the $[\text{SiSAg}]_4$ presently under investigation.

The ^{29}Si spectrum recorded at 5.87 T, presented in [1] can not be understood totally. Obviously the fine structure (5 lines) is due to $\{^{29}\text{Si}, ^{107}\text{Ag}\}$ and $\{^{29}\text{Si}, ^{109}\text{Ag}\}$ couplings. Therefore this spectrum should be remeasured.

To understand the ^{109}Ag NMR spectra containing couplings, the ^{109}Ag relaxation rates should be

known. As the silver relaxation of Ag nuclei in molecules has not been investigated up until now, it is of great interest, to determine not only the total ^{109}Ag relaxation rates but also the relaxation mechanisms contributing. To evaluate these contributions to $1/T_1$, relaxation measurements in considerably different fields B_0 and at different temperatures are required.

2. Experimental

NMR investigations were performed using two spectrometers with considerably different fields B_0 :

The ^{29}Si and the ^{109}Ag measurements at $B_0 = 9.395$ T (79.5 MHz and 18.6 MHz, respectively) were performed in Zürich on a Bruker AM-400 wide-bore spectrometer with a 20 mm broadband probehead (12–100 MHz). The ^{29}Si and ^{109}Ag spectra were recorded by applying 90° pulses with a period of 3 s and 5 s, respectively. To achieve a sufficient signal/noise ratio, 74 000 and 1320 scans, respectively, had to be averaged. No digital filtering techniques were used, to get an unbroadened line shape.

^{109}Ag T_1 values were determined by means of the inversion-recovery technique [5], and the following pulse sequence was used:

$$\{[(\pi - \tau_i - \pi/2 - \text{AT} - \text{D})_n - \text{new } \tau_i]_i (\text{D} - \pi/2)_n\}_m.$$

The parameters used for the sample described above were: spectral width 1500 Hz, acquisition time (AT) = 1.4 s, pulse delay (D) = 5 s, and the pulse sequence repetition numbers were $n = 4$ (alternating phase cycle of the receiver), $i = 9$ (corresponding to 9 points on the final T_1 plot), and $m = 32$. The temperature variation in time and the temperature gradient in the probe can be estimated < 1 K in each case. Temperature effects and changes in B_0 field homogeneity are effectively averaged by use of the above pulse repetition sequence. The data were processed with and without the equilibrium magnetization M_0 , determined by the last part of the above pulse sequence, making use of a Gaussian fitting. The consistent data were averaged for entry in Table 1.

All low field ^{109}Ag measurements were performed in Tübingen in a field $B_0 = 2.114$ T produced by a Bruker B-E 45 electromagnet externally stabilized by the Bruker NMR stabilizer B-SN 15. The spatial homogeneity $|\Delta B_0| < 10^{-6}$ T in the region of the sample (cylinder 18 mm internal diameter, 37 mm filling height) was achieved by 12-gradient electric shims. A

Table 1. Results of relaxation measurements of $[(t\text{-C}_4\text{H}_9\text{O})_3\text{SiSAG}]_4$ 0.07 M in toluene.

Temp. in K	At $B_0 = 2.114$ T			At $B_0 = 9.395$ T		$a \times 10^3$ in s^{-1}	$b \times 10^3$ in $\text{s}^{-1} \text{T}^{-2}$
	Relax. time in s T_1	Relax. time in s T_2	Relax. rate in s^{-1} $1/T_1$	Relax. time in s T_1	Relax. rate in s^{-1} $1/T_1$		
280	14.80	9.61	0.0676	0.739	1.353	-0.99 ± 3.60	15.34 ± 0.35
301	20.22	12.72	0.0495	1.101	0.908	3.66 ± 2.55	10.25 ± 0.24

Note: The relaxation times determined at $B_0 = 2$ T are affected with an uncertainty of $\pm 3\%$ and the relaxation times measured at $B_0 = 9$ T with $\pm 2\%$. The absolute uncertainty of the temperatures is ± 1 K.

“home-built” pulse-spectrometer [6] was used, especially developed for investigations of very weak NMR signals in the frequency range 1 to 4.5 MHz. The ^{109}Ag spectrum was recorded as well with the quadriga technique [7] using a pulse repetition rate of 83 Hz as by observing the free induction decay (FID) using a pulse period $T = 40 \text{ s} \gg T_2$ and the optimum flip angle $\Theta = 82^\circ$. With the steady-state technique, a signal/noise ratio of better than 60 could be attained with 2.5×10^6 pulses in a measuring time of 8 hours whereas the FID-technique required ≈ 89 hours for 8000 pulses, and yielded a signal/noise ratio of ≈ 25 .

To determine the ^{109}Ag relaxation times, steady-state techniques, which are described in detail in [8, 9] were used: Periodic, equal and coherent RF pulses were applied with a repetition rate of 83.3 Hz. Two kinds of experiments, the T_1/T_2 and the $(T_1 + T_2)$ experiment had to be combined to evaluate the desired relaxation times T_1 and T_2 . In the T_1/T_2 experiment, the dependence of the steady-state NMR signal amplitude on the applied flip angle was determined for approximately a dozen different flip angles Θ , ranging from 10° to 90° . For each such measurement an accumulation time of 6 hours was required to achieve a signal/noise of better than 50, thereby obtaining a sufficiently low uncertainty of the signal amplitudes. By a least-squares Gaussian fitting routine applied to this set of experimental data, the ratio T_1/T_2 as well as the signal amplitude corresponding to the equilibrium magnetization M_0 may be evaluated. In Fig. 2, a result of an experiment of this type is pointed out. In the $(T_1 + T_2)$ experiment, the development of the steady-state was observed during a time interval of 45 s. This period was divided into 15 segments, and the NMR signal obtained from 250 RF pulses was accumulated during each of these segments. Since such a time interval of 3 s is far too short to obtain sufficient signal/noise ratio, this experiment was repeated 10,000 times

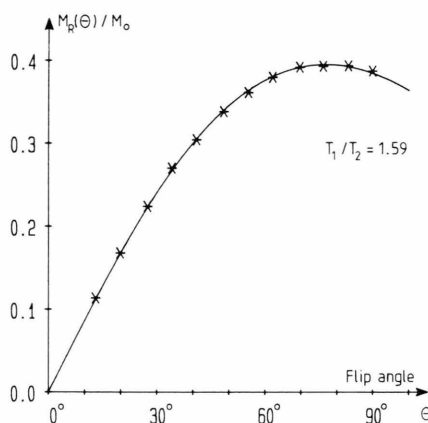


Fig. 2. Result of the ^{109}Ag T_1/T_2 -experiment at $B_0 = 2.114$ T of $[(t\text{-C}_4\text{H}_9\text{O})_3\text{SiSAG}]_4$ 0.07 M in toluene at 301 K. The steady-state signal amplitudes determined as a function of the flip angle Θ and the theoretical function with the optimum fit parameters T_1/T_2 and M_0 are plotted.

and the NMR signal was acquired during each of these 3 s intervals. To get a new well defined initial state for the next buildup of the steady-state, the transverse magnetization M_R was destroyed by the diffusion during 2 s in the homogeneity spoiled field B_0 and the longitudinal magnetization M_z was inverted by application of a π -pulse after this time interval; this steady-state inversion recovery technique [10] enables a higher dynamic range for the development of the steady-state than a demagnetization of the sample [11]. The time constant $T^* = (T_1 + T_2)/2$ of the exponential buildup of the steady-state NMR signal was evaluated by a Gaussian least-squares fitting routine from the 15 measured NMR signal amplitudes. A result of the $(T_1 + T_2)$ experiment is presented in Figure 3.

The NMR signal between RF pulses was digitized with the aid of a special “home built” ADC-card (dwell-time 5 μs /channel, resolution 8 bit) in an AT-

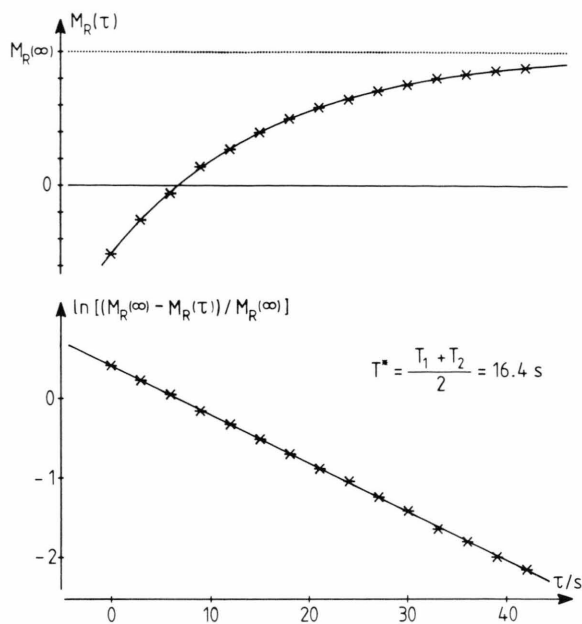


Fig. 3. Result of the ^{109}Ag ($T_1 + T_2$)-experiment at $B_0 = 2.114\text{ T}$ of $[(t\text{-C}_4\text{H}_9\text{O})_3\text{SiSag}]_4$ 0.07 M in toluene at 301 K. The exponential buildup of the steady-state after inversion of M_z and destruction of M_R was determined with a block-averaging technique as a function of the time τ elapsed since this initialization. The buildup time-constant T^* was determined by a Gaussian least squares fitting routine from the linear signal amplitudes M_R . The quality of the fit is demonstrated in the logarithmic plot.

compatible personal computer and accumulated in the memory of this computer. Block-averaging was achieved by switching the segment-register to the basis-address of a new block ($2\text{ K} \times 4$ bytes) each time after 250 RF pulses. As this switching from one memory region to the next one lasts only a few μs and no data transfer is required, the time interval of one block immediately adjoins the interval of the next block and no NMR signal is lost at all. This rapid way of block-averaging in the memory of a computer allows the determination of relatively short time constants T^* . This computer and its clock also control the pulse programmer as well as the frequency synthesizer (Schomandl MG 520 M), and the homogeneity spoil pulse. The Fourier transformation in floating point mode as well as all further evaluation was done by a PDP 11/73 computer.

The determination of the NMR signal amplitude corresponding to the equilibrium magnetization M_0 from the FID requires the knowledge of the initial NMR signal amplitude immediately after the RF

pulse. Unfortunately, during the first 2 ms after the RF pulse, the ^{109}Ag NMR signal cannot be observed because of unavoidable acoustic ringing of the sample circuit, and this missing part of the FID can not be restored by extrapolation, as the FID is not exponential, rather it is governed by the distribution of the spin isochromats, i.e. by the distribution of B_0 in the range of the sample. This missing part of the FID causes a baseline distortion after Fourier-transformation, which severely affects the maximum of the NMR line. Taking into account however, that all spin isochromats start their free precession exactly with the same phase after the RF pulse, this missing part of the FID can be restored with the aid of an iterative routine, i.e. the absorption NMR signal can be corrected exactly to that shape $I_A(\nu)$, which would be recorded without any loss of NMR signal. The integral of that absorption line corresponds to the equilibrium magnetization M_0 :

$$\int_0^\infty I_A(\nu) d\nu = C \times M_0. \quad (1)$$

In a steady-state experiment with the pulse period T and the optimum flip angle $\Theta = \arccos \{(T_1/T_2 - 1)/(T_1/T_2 + 1)\}$, between the pulses an NMR signal of constant amplitude can be received during the time interval αT ($0 < \alpha < 1$), which yields after Fourier-transformation an absorption line with the shape

$$I_A(\nu) = C \times (M_0/2) \times \sqrt{T_2/T_1} \times \sin \{2\pi\alpha T(\nu_L - \nu)\} / \{2\pi T(\nu_L - \nu)\}. \quad (2)$$

In (1) and (2), C is the same apparative constant. By this, an evaluation of M_0 is possible from both types of experiment, taking into account the different number of pulses.

The synthesis of $[(t\text{-C}_4\text{H}_9\text{O})_3\text{SiSag}]_4$ is described in detail in [1]. The sample was filtered under inert gas atmosphere directly into the sample tube of 18 mm internal diameter, degassed by five freeze-pump-thaw cycles and sealed under vacuum.

3. Results and Discussion

a) Relaxation

The knowledge of the relaxation rates and especially of the relaxation mechanisms is of central importance for the understanding of the spectra and especially of the coupling phenomena; therefore, this

point should be discussed first. Relaxation rates were determined only for the silver isotope ^{109}Ag in two different fields B_0 at two different temperatures. Up until now, ^{109}Ag relaxation rates were determined only for the solvated Ag^+ ion [12]; in this work the first ^{109}Ag relaxation investigations with a large molecule are presented. The results are given in Table 1. The relative uncertainties of $\pm 3\%$ and of $\pm 2\%$ are the standard deviations, they are mostly due to the uncertainties of the signal intensities caused by the noise and to the pulse angle missettings in the high-field measurements. In this large $[\text{SiSag}]_4$ molecule considerably shorter relaxation times T_1 were determined than for the $^{109}\text{Ag}^+$ ion, which is extremely slowly relaxing ($T_1 > 1000$ s). Such relatively high ^{109}Ag relaxation rates enable the registration of ^{109}Ag NMR spectra with the usual FID-technique even in the low field $B_0 = 2.114$ T.

The results of the longitudinal relaxation in Table 1 show a strong dependence of this relaxation rate on the field strength B_0 . The only relaxation mechanism, which is affected by the strength of the static field B_0 even in the extreme narrowing case, is chemical shift anisotropy combined with molecular reorientation (CSA) [13]. Assuming the extreme narrowing condition $\omega_L \tau_c \ll 1$ to be valid, the longitudinal relaxation rate due to CSA is

$$1/T_1^{(\text{CSA})} = \frac{1}{10} (\gamma B_0)^2 (\Delta\sigma)^2 \tau_c \quad (3)$$

in the case of a symmetric shielding tensor with the anisotropy

$$(\Delta\sigma)^2 = \sigma_x^2 + \sigma_y^2 + \sigma_z^2 - 2\sigma_x\sigma_y - 2\sigma_x\sigma_z - 2\sigma_y\sigma_z,$$

with the elements σ_i of the traceless, diagonal shielding tensor and with the correlation time τ_c for angular reorientation.

The contributions of all other relaxation mechanisms (dipole-dipole interaction (DD), scalar interaction (SC), and spin rotation (SR)) to the relaxation rates do not depend on the strength of the static field B_0 in the extreme narrowing case. Therefore the spin-lattice relaxation rate may be split into a field independent part a and a quadratically field dependent contribution $b B_0^2$:

$$1/T_1 = a + b B_0^2. \quad (4)$$

From the results of the longitudinal relaxation rates determined at considerably different fields B_0 , as pointed out in Table 1, the constants a and b can be

calculated with the aid of (4). The results for different temperatures are given in the last two columns of Table 1. For both static fields used ($B_0 = 2.114$ T and $B_0 = 9.395$ T) the relation $a \ll b B_0^2$ is valid, i.e. CSA is the by far dominant relaxation mechanism. The contribution of the field independent relaxation mechanisms (DD, SC, and SR) to the total relaxation rates is extremely weak; in the high field, this contribution is far below the experimental uncertainty of the measured relaxation rates, whereas in the low field, at least at 301 K, a significant contribution of 7.4% to the rate $1/T_1$ was determined. At 280 K, the interval of uncertainty of the constant a includes the value 0 (of course, negative values of a , i.e. negative contributions to the relaxation rate are, not possible!); this shows that a significant field independent contribution to the longitudinal relaxation rate could not be detected at that temperature. The field independent contribution to the spin-lattice relaxation rate $1/T_1$, i.e. the constant a , seems to increase with increasing temperature. This behaviour is characteristic for the SR mechanism [14, 15], i.e. among the field independent relaxation mechanisms, SR yields the dominant contribution to the longitudinal relaxation rate. Because of this small field independent relaxation rate and its high relative statistic uncertainty, no attempt was made to separate contributions by the DD and SC mechanisms, which decrease with increasing temperature.

In the low field $B_0 = 2.114$ T also the transverse relaxation times T_2 were determined. At both temperatures, the ratio $T_1/T_2 \approx 1.6$ was measured. For the relaxation mechanism CSA the theoretical ratio $T_1/T_2 = 7/6$ was pointed out for the case of a symmetric shielding tensor [13]; in the case of an antisymmetric part of this tensor, a ratio $T_1/T_2 \leq 7/6$ was predicted [16], i.e. the measured ratio T_1/T_2 can not be explained by a low point symmetry of the Ag atoms under investigation in the $[\text{SiSag}]_4$.

Although there are scalar couplings of the silver nuclei under investigation to the neighbouring ^{33}S nuclei and also to the ^{29}Si nuclei, the mechanism of scalar coupling of the second kind [17] surely does not contribute to the spin-lattice relaxation rate $1/T_1$ as the Larmor frequencies of ^{33}S and of ^{29}Si are considerably different from that of ^{109}Ag ; however a contribution to the transverse relaxation is possible if the condition $|J(^{109}\text{Ag}, \text{A})| \times T_1(\text{A}) \ll 1$ is fulfilled:

$$1/T_2^{\text{SC}}(^{109}\text{Ag}) = \frac{4\pi^2 [J(^{109}\text{Ag}, \text{A})]^2}{3} S(S+1) T_1(\text{A})$$

with the spin S and the longitudinal relaxation time $T_1(A)$ of nucleus $A = {}^{33}\text{S}$ or ^{29}Si . In the low field $B_0 = 2.114\text{ T}$ a contribution from the $\{^{109}\text{Ag}, {}^{29}\text{Si}\}$ coupling may surely be excluded as the product $|J| \times T_1({}^{29}\text{Si}) \approx 5$ will be evaluated below, however the nucleus ^{33}S with the spin $I = 3/2$ should give a considerable SC contribution to the transverse relaxation rate of ^{109}Ag because of its rapid relaxation due to the quadrupole moment and because of the probably stronger scalar coupling to ^{109}Ag . In the natural mixture the only magnetic sulphur nucleus ^{33}S has an abundance of only 0.76%, this means that only 1.51% of the ^{109}Ag nuclei under investigation are coupled to ^{33}S . Probably the ratio T_1/T_2 of these ^{109}Ag nuclei is extremely high due to the $1/T_2^{\text{SC}}$ contribution, and this may be the reason why they do not contribute to the ^{109}Ag steady-state NMR signal [18] and that they do not affect the relaxation investigations. Any SC contribution to the ^{109}Ag transverse relaxation would affect only a part of the silver nuclei (1.51% are coupled to ^{33}S and 9.34% to ^{29}Si) and this part would give different results in the relaxation experiments; the results as well of the T_1/T_2 experiment, given in Fig. 2, as of the $(T_1 + T_2)$ experiment, demonstrated in Fig. 3, do not give any hint for two different ratios T_1/T_2 or for two different built-up time constants T^* , respectively. Therefore SC may be excluded as mechanism to explain $T_1/T_2 \approx 1.6$.

Rather a rapid chemical exchange must be assumed as a reason [19, 20] for the measured ratio T_1/T_2 , as only the transverse relaxation rate is increased by such an exchange and not the longitudinal one. This exchange mechanism could be a short lived adsorption of the molecule under investigation to a colloidal silver particle in the sample or an exchange in the solvation shell of the $[\text{SiSAg}]_4$ molecule as it was pointed out for the silver ion [12]. But it must be expressed clearly that neither a transient development of the relaxation rate $1/T_2$ nor a significant amount of Rayleigh scattered light, as it was found for the silver ion in aqueous solution [12], was to be detected in the present investigations of the $[\text{SiSAg}]_4$ molecule dissolved in toluene.

As ^{29}Si is the only magnetic Si isotope (4.7% natural abundance) and has the spin $I = 1/2$ and a relatively small magnetic moment like ^{109}Ag , the ^{29}Si relaxation should be governed by the same mechanisms as the ^{109}Ag relaxation, i.e. CSA should also be the predominant ^{29}Si relaxation mechanism. Of course, the magnetic shielding tensor for the Si atoms

in the $[\text{SiSAg}]_4$ molecule is different from that for the Ag nuclei. With the same chemical shift anisotropy $\Delta\sigma$ for the ^{29}Si as for the ^{109}Ag nuclei, according to (3), the spin-lattice relaxation rates of ^{29}Si and ^{109}Ag should behave like the squares of the gyromagnetic ratio $(\gamma({}^{29}\text{Si})/\gamma({}^{109}\text{Ag}))^2 = 18.18$. Assuming chemical shift anisotropies $\Delta\sigma$ of the same order of magnitude for ^{29}Si as for ^{109}Ag , the ^{29}Si relaxation times may be estimated to be about one order or magnitude shorter than those of ^{109}Ag .

b) ^{109}Ag and ^{29}Si NMR Spectra

The ^{109}Ag spectrum was recorded as well at $B_0 = 2.114\text{ T}$ as on the high field spectrometer at $B_0 = 9.395\text{ T}$, in both spectrometers at a temperature of 300 K. At both field strengths, only a single NMR line without any fine structure was to be detected. In the low field spectrometer, the ^{109}Ag line recorded with the FID technique had a halfwidth $\Delta\nu \approx 4\text{ Hz}$ and its shape was due to the distribution of the field B_0 , whereas the line taken with the Quadriga technique was artificially broadened by saturation to a halfwidth $\Delta\nu \approx 50\text{ Hz}$, in order to get the optimum signal intensity; the shape of this steady-state line is described by (2). Even in the high field spectrometer with the shorter relaxation times, as pointed out in Table 1, the width of the ^{109}Ag NMR line $\Delta\nu = 4.5\text{ Hz}$ was mostly due to inhomogeneous broadening by the spectrometer.

At the low field $B_0 = 2.114\text{ T}$ using the steady-state technique the ratio of the Larmor frequencies of ^{109}Ag in $[\text{SiSAg}]_4$ 0.07 M in toluene and of ^{73}Ge in GeCl_4 was determined with the aid of the sample replacement technique. Both samples had the same size and shape and were measured at 300 K. The result is

$$\nu({}^{109}\text{Ag})/\nu({}^{73}\text{Ge}) = 1.3349877 \pm 0.0000002.$$

The ^{73}Ge resonance of the neat liquid GeCl_4 is a well known standard for low- γ nuclei [21]. Referred to the Larmor frequency of the Ag^+ ion in aqueous solution at infinite dilution [22], the ^{109}Ag resonance of the $[\text{SiSAg}]_4$ sample is shifted to higher frequency at the same field B_0 by

$$\delta = (725.8 \pm 1.5)\text{ ppm}.$$

The ^{29}Si spectrum was recorded only in the high field spectrometer. This spectrum is presented in Figure 4a. Obviously this spectrum shows a not fully resolved fine structure due to a scalar coupling of ^{29}Si

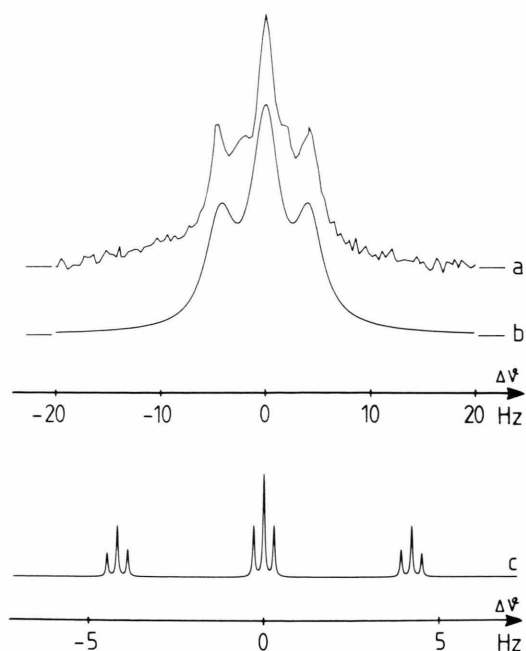


Fig. 4. a) ^{29}Si spectrum at $B_0 = 9.395$ T of $[(t\text{-C}_4\text{H}_9\text{O})_3\text{SiAg}]_4$ 0.07 M in toluene at 300 K recorded within ≈ 62 hours; no digital filtering techniques were applied in order to enable a Gaussian fit. b) Theoretical ^{29}Si spectrum with the optimum fit parameters for $|J(^{29}\text{Si}, ^{109}\text{Ag})|$ and $T_2(^{29}\text{Si})$. c) Fully resolved theoretical ^{29}Si spectrum with the fictitious transverse relaxation time $T_2(^{29}\text{Si}) = 5$ s. This fine structure is due to scalar coupling of ^{29}Si to ^{107}Ag and ^{109}Ag in natural abundance. The changed abscissa scale should be regarded.

to the two neighbouring Ag nuclei as suggested by the intensity ratio $\approx 1:2:1$. As silver has two magnetic isotopes ^{107}Ag and ^{109}Ag both with the spin $I = 1/2$ and nearly equal natural abundance of 51.82% and 48.18%, respectively, the couplings to the two silver isotopes must be considered separately. As the ^{29}Si is only 4.7% abundant in the natural mixture, solely $[\text{SiAg}]_4$ molecules with one ^{29}Si nucleus must be regarded; molecules with two or more ^{29}Si nuclei are so much improbable (1.2%) that their ^{29}Si NMR signal is below the noise. 26.85% of the ^{29}Si nuclei have two neighbouring ^{107}Ag nuclei and 23.21% of the ^{29}Si nuclei are coupled to two ^{109}Ag nuclei, whereas 49.93% of the ^{29}Si nuclei are coupled to two different silver isotopes; therefore three types of theoretical ^{29}Si spectra must be superimposed to get the experimental spectrum plotted in Figure 4a. Taking into account the ratio of the couplings constants

$$\begin{aligned} J(^{29}\text{Si}, ^{107}\text{Ag})/J(^{29}\text{Si}, ^{109}\text{Ag}) &= \gamma(^{107}\text{Ag})/\gamma(^{109}\text{Ag}) \\ &= 0.870, \end{aligned}$$

the total ^{29}Si spectrum may be calculated, assuming Lorentzian line shapes; the Ag relaxation may be neglected in this consideration, as the Ag relaxation rates are smaller at least by an order of magnitude than those of ^{29}Si as estimated above. The experimental ^{29}Si spectrum was fitted with the aid of a Gaussian least squares fitting routine, the following results for the fit parameters were obtained: the coupling constants

$$|J(^{29}\text{Si}, ^{109}\text{Ag})| = (4.49 \pm 0.04) \text{ Hz},$$

$$|J(^{29}\text{Si}, ^{107}\text{Ag})| = (3.90 \pm 0.03) \text{ Hz},$$

and the transverse relaxation time

$$T_2(^{29}\text{Si}) = (103 \pm 2) \text{ ms}.$$

In Fig. 4b the ^{29}Si spectrum calculated with these optimum fit parameters is plotted, whereas in Fig. 4c, the ^{29}Si spectrum calculated with $T_2(^{29}\text{Si}) = 5$ s (this is the transverse relaxation time in a field $B_0 = 1.3$ T, assuming CSA to be the only relaxation mechanism) is plotted in order to point out its fine structure. Different isotopic shifts of the ^{29}Si resonance due to the silver isotopes ^{107}Ag and ^{109}Ag were not taken into account as the experimental spectrum was not asymmetric within the limits of error due to the noise superimposed.

c) Silver-Silver Couplings

Based on the symmetry of the $[\text{SiAg}]_4$ molecule, all four silver atoms are equivalent atoms. This symmetry, however, is disturbed because of the isotopic mixture of Ag, which consists of the isotopes ^{107}Ag and ^{109}Ag , nearly with the same natural abundance (51.82% and 48.18%, respectively). Regarding only the silver isotopes, six different types of $[\text{SiAg}]_4$ molecules are possible, changing the isotopes of the four silver atoms in the central squared ring. Two types of scalar $\{\text{Ag}, \text{Ag}\}$ couplings are imaginable: a coupling to the vicinal silver atom directly or through the S atom at the corner of the square and possibly a scalar coupling directly to the silver atom at the opposite site of the central square of the $[\text{SiAg}]_4$ molecule. The latter kind of $\{\text{Ag}, \text{Ag}\}$ coupling should be taken into account because of the spatial shift of the Ag atoms towards the centre of the ring. In Table 2, all types of couplings of an ^{109}Ag nucleus with the three other silver nuclei in the central ring and their relative quota are listed. Pure homonuclear couplings $\{^{109}\text{Ag}, ^{109}\text{Ag}\}$ as well as pure heteronuclear couplings

Table 2. Possible couplings of ^{109}Ag nuclei under investigation in the $[(t\text{-C}_4\text{H}_9\text{O})_3\text{SiSag}]_4$ molecule to other silver nuclei.

Quota of ^{109}Ag in %	Coupled to		
	vicinal	vicinal	opposite
11.51	^{109}Ag	^{109}Ag	^{109}Ag
12.15	^{109}Ag	^{109}Ag	^{107}Ag
24.30	^{109}Ag	^{107}Ag	^{109}Ag
25.66	^{109}Ag	^{107}Ag	^{107}Ag
12.83	^{107}Ag	^{107}Ag	^{109}Ag
13.55	^{107}Ag	^{107}Ag	^{107}Ag

$\{^{109}\text{Ag}, ^{107}\text{Ag}\}$ are relatively rare, whereas most of the ^{109}Ag nuclei are coupled as well to ^{109}Ag as to ^{107}Ag .

Such $\{^{109}\text{Ag}, \text{Ag}\}$ couplings of the same strength as the $\{^{109}\text{Ag}, ^{29}\text{Si}\}$ couplings in Fig. 4, would yield well resolved multiplets in the ^{109}Ag spectrum recorded in the high resolution spectrometer at $B_0 = 9.395$ T. Fortunately, the Ag relaxation times are longer by at least one order of magnitude than those of ^{29}Si and for this reason the Ag NMR lines should be more narrow by this factor than the ^{29}Si lines. This should enable the detection of $\{\text{Ag}, \text{Ag}\}$ couplings with coupling constants $|J| \geq 1.5$ Hz, but not any hint for such an $\{\text{Ag}, \text{Ag}\}$ coupling can be taken from the ^{109}Ag spectrum.

The steady-state technique offers an additional, very sensitive way to detect homonuclear couplings. The steady-state signal amplitude is reduced considerably by a homonuclear coupling with $T \times |J| \geq 1\%$ [23]. To do this test, the equilibrium magnetization M_0 was determined from the maximum of the absorp-

tion resonance curve as described in (2), and on the other hand M_0 was determined from the corrected FID absorption signal with the aid of (1). The experimental result for the ratio of the equilibrium magnetization determined in different ways is

$$M_0(\text{St.-St.})/M_0(\text{FID}) = 97.1\%.$$

Taking into account, that the steady-state signal is also affected by heteronuclear coupling [24]: 1.51% of the ^{109}Ag nuclei coupled to ^{33}S do not contribute to the steady-state signal as demonstrated above, but they do contribute to the initial amplitude of the FID; all ^{109}Ag nuclei coupled to ^{29}Si (9.3%) will give a contribution of only 95% to the steady-state signal (calculated in the way outlined in [24] under the assumption $T_1(^{29}\text{Si})/T = 100$), whereas they contribute fully to the initial FID amplitude. Without any $\{^{109}\text{Ag}, ^{109}\text{Ag}\}$ coupling, the ratio should become

$$M_0(\text{St.-St.})/M_0(\text{FID}) = 98.0\%.$$

Taking into account the experimental uncertainties, this value coincides fully with the experimental result; i.e. reduction of the steady-state signal due to homonuclear $\{^{109}\text{Ag}, ^{109}\text{Ag}\}$ coupling may be excluded. Therefore the coupling constants of any $\{\text{Ag}, \text{Ag}\}$ coupling are surely $|J(\text{Ag}, \text{Ag})| < 1$ Hz.

This result clearly points out, that the assumption of any binding interaction between the Ag atoms in the $[\text{SiSag}]_4$ molecule is very doubtful. This result should be transferable to the isomorphous copper compound $[\text{SiScu}]_4$, which can not be investigated in the same way because of the quadrupole moment of both copper isotopes.

- [1] W. Wojnowski, M. Wojnowski, K. Peters, E.-M. Peters, and H. G. von Schnering, *Z. anorg. al. Chem.* **530**, 79 (1985).
- [2] B. Becker, W. Wojnowski, K. Peters, E.-M. Peters, and H. G. von Schnering, *Polyhedron* **9**, 1659 (1990).
- [3] M. Jansen, *J. Less-Common Met.* **76**, 285 (1980).
- [4] S. S. D. Brown, I. J. Colquhoun, W. McFarlane, M. Murray, I. D. Salter, and V. Sik, *J. Chem. Soc., Chem. Commun.* **1986**, 53.
- [5] H. Y. Carr and E. M. Purcell, *Phys. Rev.* **94**, 630 (1954); M. L. Martin, J. J. Delpuech, and G. J. Martin, *Practical NMR Spectroscopy*, p. 246 f., Heyden, London 1980.
- [6] A. Schwenk, *Z. Phys.* **213**, 482 (1968).
- [7] A. Schwenk, *J. Magn. Reson.* **5**, 376 (1971).
- [8] J. Kronenbitter and A. Schwenk, *J. Magn. Reson.* **25**, 147 (1977).
- [9] A. Schwenk, *Progr. NMR Spectrosc.* **17**, 69 (1985).
- [10] W. Kreibich and A. Schwenk, 9th European Experimental NMR Conference, May 16–20, 1988 "Program and Abstracts", p. 160; will be published in detail.
- [11] W. Kreibich and A. Schwenk, *J. Magn. Reson.* **77**, 308 (1988).
- [12] H. Pfister, A. Schwenk, and D. Zeller, *J. Magn. Reson.* **68**, 138 (1986).
- [13] A. Abragam, *The Principles of Nuclear Magnetism*, p. 315 f., Oxford Univ. Press, New York, London 1961.
- [14] P. S. Hubbard, *Phys. Rev.* **131**, 1155 (1963).
- [15] H. W. Spiess, *Rotation of Molecules and Nuclear Spin Relaxation in "NMR Basic Principles and Progress"* (P. Diehl, E. Fluck, and R. Kosfeld, Eds.), Vol. 15, Springer-Verlag, Berlin 1978.
- [16] see Ref. [15], p. 118.
- [17] see Ref. [13], p. 309 f.
- [18] see Eq. (2.14) in Ref. [9].
- [19] S. Meiboom, *J. Chem. Phys.* **34**, 375 (1961).
- [20] A. Allerhand and H. S. Gutowsky, *J. Chem. Phys.* **41**, 2115 (1964).
- [21] W. Sahm and A. Schwenk, *Z. Naturforsch.* **29a**, 1763 (1974).
- [22] C.-W. Burges, R. Koschmieder, W. Sahm, and A. Schwenk, *Z. Naturforsch.* **28a**, 1753 (1973).
- [23] see Sect. 5.2 of Ref. [9].
- [24] see Sect. 5.1 of Ref. [9].